Engineering and Technology Journal
Journal homepage: https://etj.uotechnology.edu.iq

Effects of aging, temperature, and time on the ultimate tensile strength of Al 2024

Benedict U. Iyida[a], **Azubuike M. Nwankwo**[b*], **Thomas O. Onah**[c]

[a] Mechanical Engineering Dept., Caritas University, Amorji-Nike, Enugu, Nigeria.
[b] Division of Works Engineering Services, Federal Polytechnic, Oko Anambra State, Nigeria.
[c] Mechanical and Production Engineering Dept., Enugu State University of Science and Technology, Enugu, Nigeria.
*Corresponding author Email: zubbymike@gmail.com

HIGHLIGHTS

- Aging temperature and time effects on the ultimate tensile strength of Al2024 were examined.
- Optical microstructure analysis was used at different times, including as-quenched and as-cast conditions.
- The ultimate tensile strength of Al2024 increased by up to 175.7% after heat treatment, quenching, and artificial aging.

Keywords:
Al 2024
Ageing Temperature
Ageing Time
Ultimate Tensile Strength
Elongation

ABSTRACT

This study focuses on the ultimate tensile strength of Al 2024 in that since the past decade, Al 2024 alloy (Al-4.5% Cu-1.5% Mg-0.6% Mn) has been one of the most widely used Al-Cu-Mg-Mn alloys. Therefore, it was subjected to heat treatment, quenching, and artificial aging. The artificial aging temperatures were 1400 °C, 1600 °C, 1800 °C, and 1900 °C, each for the range from 0.5 hr to 9 hr. The ultimate tensile strength of the as-cast after solutionizing and quenching increased from 185 MPa to 199 MPa, representing a 7.6% increase. At 1900 °C aging temperature, the peak value of 348 MPa, representing an 88.1% increase from the as-cast value, was recorded at 6 hr aging time. The drops in ultimate tensile strength values outside the peak aging time of 6 hr were attributed to the precipitation of incoherent and coarse secondary phases in the alloy structure. Ultimate tensile strength values increased at various aging temperatures and aging times, culminating in 482 MPa, which is the semi-maximum overall value at 1800 °C and 6 hr. Aging temperature, representing a 160.5% increase from the as-cast value, while 510 MPa was recorded as the overall maximum ultimate tensile strength at 1400 °C and 8 hr aging time, representing a 175.7% increase from the as-cast value. This was a very considerable enhancement in the mechanical properties of Al 2024 with respect to ultimate tensile strength.

1. Introduction

The Al 2024, made up of Al-4.5%Cu-1.5%Mg-0.6%Mn, has been widely used over the years as an Al-Cu-Mg-Mn alloy. It has received great attention in terms of usage due to its excellent strength-to-density ratio, formability, corrosion resistance, good fracture toughness, and excellent fatigue resistance properties [1,2]. Oguocha [3] showed that Al alloys have good formability in their 'zero' condition, but like any heat-treatable alloy, it has poor weldability.

This alloy has been considered a substitute for steel materials used in automobile, aerospace, electrical, and cable industries for the production of aircraft rivet structure hardware, truck wheels, screw machine products, etc. Meanwhile, its excellent performance increases at a temperature below 100 °C, and its excellent mechanical properties decrease significantly when it is exposed to temperatures above 1000 °C [4]. This difference in performance is a result of the incomplete solution mix of the solute elements with large-sized and sparsely dispersed inter-metallic compounds or precipitates in the aluminum matrix [5].

A known fact is that heat treatment of metals is generally employed to improve their mechanical properties. Still, for aluminum alloys, heat treatment is restricted to specific operations employed to increase the strength and hardness of precipitation-hardenable wrought and cast alloys. Davies [6], showed that Al 2024 is a "heat-treatable" alloy because it can obtain significant strengthening effects by heat treatment. Therefore, in order to obtain Al 2024 with the optimum combination of excellent mechanical properties, it is commonly subjected to heat treatment, quenching, and artificial aging treatment since it has a positive response to artificial aging [7]. Xu et al. [8], showed that Al 2024 possesses an enhanced strength when

http://doi.org/10.30684/etj.2025.154927.1841
Received 01 November 2024; Received in revised form 12 January 2025; Accepted 16 January 2025; Available online 10 March 2025
2412-0758/University of Technology-Iraq, Baghdad, Iraq

exposed to heat treatment because of the precipitation of the Al2CuMg phase upon solutions and artificial aging. Alexopoulos and Pantelakis [9,10], indicated that chemical composition, solidification rate, and heat treatment are the key parameters necessary for the improvement of the mechanical properties of Al 2024. Polmear [11], established that precipitation, hardened by the formation of S-type particles in the alloy - Al_2CuMg, is observed in the aluminum matrix. Also, the deformation and fracture of the alloy are affected by the size, morphology, distribution of Al-grains, and possible defects like voids, porosity, etc. He added that the presence of the secondary precipitation hardening particles is also one of the main factors contributing to the enhancement of the mechanical properties and behavior of the alloy. According to Smoljan [12], fractured toughness and fatigue limit depend on the micro-structural constituents and distribution of the inter-metallic particles and non-metallic inclusions. As well Xu et al. [8], established that precipitation-strengthened alloys show decreased positive mechanical properties in the weld zone because of the dissolution and growth of strengthening precipitates in the thermal cycle.

The Precipitation hardening heat treatment emerged as a result of the desire in automobile, transportation, and aeronautical industries to develop new materials with high strength-weight ratio, excellent ductility, and hardness [7]. It is the most common heat treatment method applied to Al 2024. The sequence of precipitation hardening heat treatment practice includes solution heat treatment at a high temperature (about 5500 °C), quenching in water, and aging (which may be either natural aging or artificial aging). On this kind of heat treatment, Jiang et al. [13], showed that solution heat treatment is most effectively carried out near the solidus where the maximum solubility exists and diffusion rates are rapid and possible to improve the fracture toughness by dissolution and modification of the soluble inter-metallic particles. It involves heating the alloy to a temperature where a single phase can be obtained and held at this temperature for a sufficient time 30 minutes to enable complete dissolution of the phase and random dispersion of the solute atoms in the solid solution [6] and [14]. Quenching (or rapid cooling in water) after solution treatment is a very critical step necessary to retard the diffusion process of the alloying elements in solid solution [6] and [14]. Quenching is to obtain a solid solution supersaturated with solute elements. The solid solution of Al 2024 at a high solutioning temperature of 5500 °C is quenched down to room temperature with the solute precipitate trapped in super-saturated and meta-stable conditions. As a result of the quench, a supersaturated solution now exists between the solute and the aluminum matrix, and an undesirable concentration of the alloying elements in the defect and grain boundary structure is avoided. According to Totten et al. [15], the alloy must be cooled rapidly to avoid solid diffusion and precipitation of the phase. The rapid quenching creates a saturated solution and allows for increased hardness, improved strength, and other mechanical properties of the material [16]. The coherent lattice phenomenon usually induces an improvement in strength. Thus, the distortion of the coherency of the migrated solute atoms with the matrix lattice structure results in interference and impediment to the movement of dislocations. This increases the ultimate tensile strength during the aging process, as opined by Iyida et al., [17]. Thermal stresses are typically minimized by reducing the cooling rate from the solutionizing temperature, as revealed by Rollanson [18]. However, if the cooling rate is too low, undesirable grain boundary precipitation will result. If the cooling rate is too high, distortion will occur, as revealed by Belhocine and Bouchetara [19]. Therefore, one of the primary challenges in quench process design is to select quenching conditions that optimize strength while minimizing distortion and, at the same time, ensuring that other undesirable properties, such as inter-granular corrosion and cracks, are not obtained, as stated by [6], [20] and [14].

This work aims to produce an Al 2024 alloy with better ultimate tensile strength and other mechanical properties. The excellent mechanical properties of Al 2024 decrease significantly when it is exposed to temperatures above 1000 °C, creating the need to identify and/or produce an aluminum alloy that can operate at elevated temperatures. After properly aging at suitable temperatures and without over-aging, it will consequently produce Al 2024, which finally establishes the effects of aging temperature and time on the ultimate tensile strength of Al 2024.

2. Materials and method

Aluminum wire, copper wire, magnesium, and manganese powders were used as the base materials. Other materials were emery paper, o-grits sizes, aluminum oxide powder, etchants (acidified ferric oxide), and water. The equipment used was a bailout crucible, muffle furnace, hack saw, weighing balance, and steel. Others are heat gun machine (Bosch GHG660LCD), tensile strength tester (100KN JPL, 130812), digital motorized Brinell hardness tester (Phase II 900-355, equipped with 20X optical microscope), digital impact strength tester (UI820), optical microscope (L2003A), digital camera, scanning electron microscope (Carl Zeiss EVO/NA10), electronic weighing balance (GF-203A) and lathe machine. Aluminum and copper wires were sourced from Curtix Cable PLC, while magnesium and manganese powders were supplied by Sigma-Aldrich PLC, both in Nnewi, Anambra State, Nigeria. Table 1 shows the compositions of the four Elements that make up the Al 2024 alloy: Aluminum, Copper, Manganese, and magnesium.

2.1 Experimental design

A full-factorial two-level design was used to design the experiment, considering two dependent factors: aging temperature and aging time. This was used basically to determine simultaneously the individual and interactive effects of the factors that hopefully will affect the output results [21]. The actual coded values of the factors and the design layout in standard order are presented in Tables 2 and 3, respectively.

As artificial aging was adopted, 140 °C was chosen as the low-level aging temperature because the aging temperature should not be too close to room temperature to ensure that fine precipitation occurs inside the grain boundaries. Correspondingly, 190 °C was chosen as the high-level aging temperature because aging temperatures should not be too close to

the solidus temperature (of 550 °C) to avoid burning, which leads to melting and oxidation at the grain boundaries. That condition seriously causes a decrease in ductility [22, 23]. Hence, the aging temperature range was from 140 °C to 190 °C.

Table 1: Composition of the constituent elements of Al 2024 Alloy

S\N	Elements	Compositions	Percentage
1	Aluminum	Aluminum Al	99.5
		Copper Cu	0.5
2	Copper	Copper C11000	99.5
		Impurities less than 50 ppm	0.5
3	Magnesium	Magnesium-24	79
		Magnesium -25	10
		Magnesium -26	11
4	Manganese	Pyrolusite MnO_2	63
		Psilomelane manganese oxide	31
		Manganife MnO_3	5

2.2 Alloy preparation and casting

The equivalent weight in grams of each element in the alloy composition was calculated using the weight percentage calculation Equation (1) and measured using the electronic weighing balance.

$$\%_{weight}/_{weight} = \frac{mass\ solute\ (g)}{mass\ solution\ (g)}\ x\ 100 \quad (1)$$

The materials were stored for the melting process. During melting, the bail crucible furnace was preheated for two minutes, and the measured pure aluminum wire was introduced into the furnace. Aluminum melt was obtained at 660 °C and then superheated to 700 °C to increase its fluidity [23]. Then, the alloying elements of copper, magnesium, and manganese were introduced into the liquid metal and stirred. The magnesium and manganese powders were wrapped in aluminum foil before being introduced into the liquid melt to avoid agglomeration and loss of materials. The mixture was stirred again after 5 minutes for complete homogeneity and then cast in a preheated permanent mold with cavity dimensions of 250 x 16 mm^2 [24] [25]. After 1.6 to 2.4 minutes, the mold was disengaged to remove the solidified cast sample. The cast sample was cleaned and machined to the appropriate dimensions using the lathe machine. Table 2 presents the normal weight composition in the parentage of the Al 2024 matrix. Though, Table 1 presents the percentage of each element, and Table 2 presents the weight of each element.

Table 2: Normal Composition Weight Percent of Al 2024 Material Matrix

Materials	Cu	Mn	Mg	Al
Percentage (g)	0.4	0.15	0.8	Balance

2.3 Characterization of alloys

A permanent die-casting technique was adopted as in their work [25]. The mold was prepared using a thick steel plate measuring 300 x 30 mm^2. A cavity of dimensions 250 x 16 mm^2 was drilled at the centre of the steel plate using a drilling machine. The steel plates were sectioned vertically into two parts at the centre, after which a dome and pin were created at the sectioned parts for easy coupling and disengagement of the mold after casting.

The aging heat treatment process was carried out using the muffle furnace, which comprised solution heat treatment at 550 °C for 2 hours, quenching in water, and then artificially aging at temperatures of 140 °C, 160 °C, 180 °C, and 190 °C for 0.5 hr, 1 hr, 2 hr, 3 hr, 4 hr, 5 hr, 6 hr, 7 hr, 8 hr, and 9 hr, respectively [26].

Figure 1 above shows the graphical representation of the aging treatment of the Al 2024 process. It starts with the initial solutionizing process, where it is heated to 550 °C. Then, there are four aging temperatures and times, all of which are the same, 0.5hr to 9 hr for the aging temperatures.

Finally, the samples were ground with emery paper. The tensile strength of the samples was characterized using the tensile testing machine. During the testing operation, the specimen was clamped at the ends of the dome-shaped sample on the fixed and movable jaws of the machine, and the tensile load was applied automatically by pressing the “down button” on the machine scale until the specimen fractured. The values of the load and extension at rupture were recorded as shown on the load scale, and the Ultimate Tensile Strength (UTS) was determined using Equation (2):

$$UTS = \frac{MAX.Fore\ (N)}{Original\ C.S.A.(mm^2)} = \frac{P_{Max}}{A} \quad (2)$$

Let UTS after casting = UTS_{cast} and UTS after quenching = UTS_{quench} then,

$$change\ in\ UTS_{quench} = UTS_{quenchchange} \quad (3)$$

$$UTS_{quenchchange} = \frac{UTS_{quench} - UTS_{cast}}{UTS_{cast}} \times 100 \quad (4)$$

Also, let UTS after ageing = UTS_{aged}, then,

$$Change\ in\ UTS_{aged} = UTS_{agedchange} \quad (5)$$

$$UTS_{agedchanged} = \frac{UTS_{aged} - UTS_{cast}}{UTS_{cast}} \times 100 \quad (6)$$

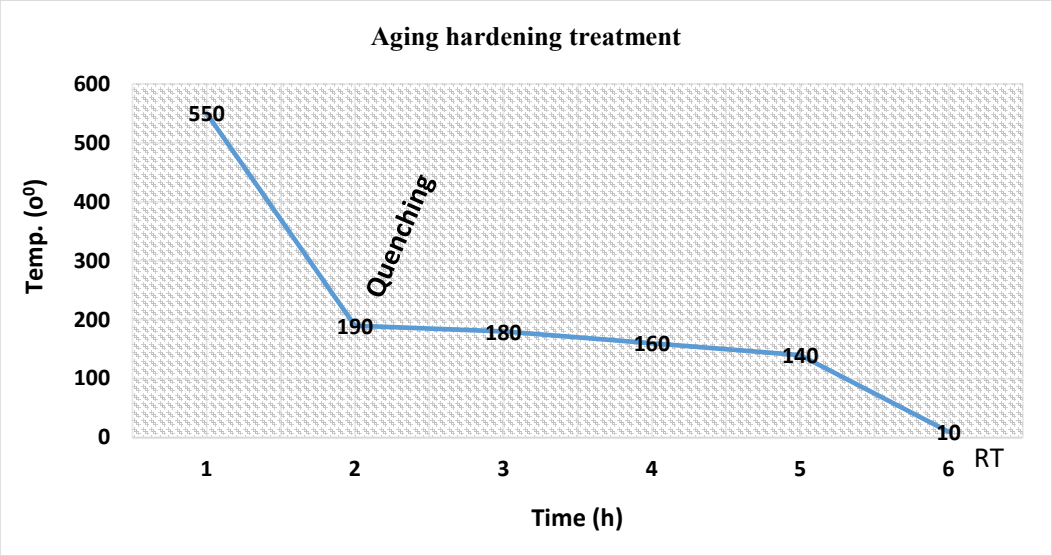

Figure 1: Schematic graph of aging hardening treatment of Al 2024 Alloy process

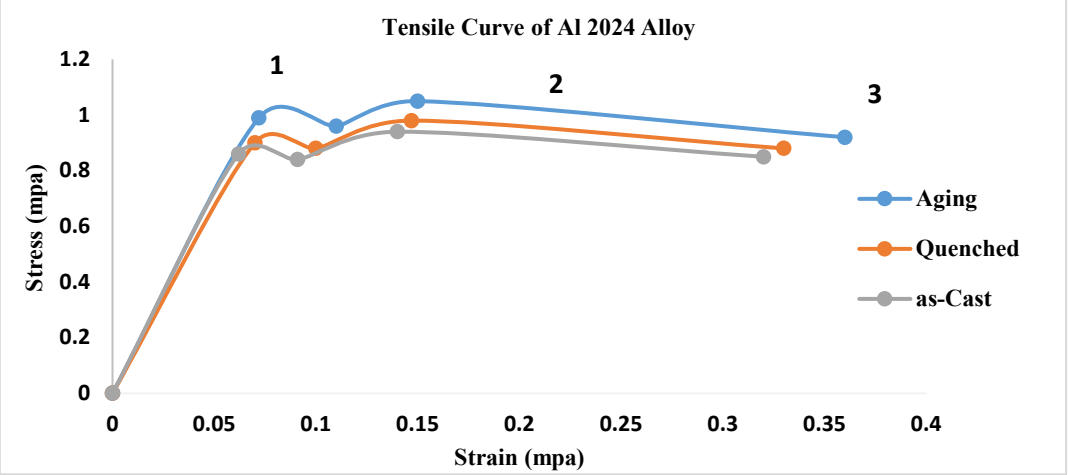

Figure 2: Tensile curve for Al 2024 As-cast, quenched, and aging specimens

Experimental data obtained from the test results were analyzed by plotting a series of curves for each test. Each series ran for a particular temperature over several aging times. Finally, a combined plot of all the values for all the temperatures was done as a correlation to display the optimal value.

The tensile curve of Figure 2 shows the ductile nature of Al 2024 material as it obeys Hookes law for ductile materials. Stress is the ratio of the applied load to the cross-section. Strain: The ratio of the change in length and original length and the ratio of stress and strain will give us the Young modulus of the Al 2024 as well as the slope of the above curve in Figure 2. Point one is the yield point, between point one and point two is the ultimate tensile strength and point 3 is the fracture point, the point of breakage. Aged treated specimen showed an increase in ultimate tensile strength.

2.4 Results and discussion

Table 3 presents the actual and coded values of the independent variables from the experiment. This table houses the aging temperature and time. Table 4 presents the design layout of aging temperature and aging time in hours and Celsius, respectively, with 42 experimental runs.

Table 3: Actual and coded values of the independent variables

Factors	Units	Low Level (-)	High Level (+)
Ageing temperature	°C	140	190
Ageing time	hr	0.5	9

Table 4: Design layout

S/N	Aging Temperature (°C)	Aging Time (hr.)
1	As – cast	-
2	Solutionized and Quenched	-
3	140	0.5
4	160	0.5
5	180	0.5
6	190	0.5
7	140	1
8	160	1
9	180	1
10	190	1
11	140	2
12	160	2
13	180	2
14	190	2
15	140	3
16	160	3
17	180	3
18	190	3
19	140	4
20	160	4
21	180	4
22	190	4
23	140	5
24	160	5
25	180	5
26	190	5
27	140	6
28	160	6
29	180	6
30	190	6
31	140	7
32	160	7
33	180	7
34	190	7
35	140	8
36	160	8
37	180	8
38	190	8
39	140	9
40	160	9
41	180	9
42	190	9

Table 5 includes the aging temperature, aging time, calculated percentage elongation, and ultimate tensile strength for the 42 experimental runs.

Table 5: Effects of ageing temperature and time on the percentage elongation and ultimate tensile strength of Al 2024

S/N	Aging Temperature (°C)	Ageing Time (hr.)	%Elongation (%)	Ultimate Tensile Strength (MPa)
1	As - cast	-	18.8	185
2	Solutionized and Quenched	-	12.7	199
3	140	0.5	17.9	205
4	160	0.5	15.8	360
5	180	0.5	14.8	216
6	190	0.5	14.6	209
7	140	1	17.1	278
8	160	1	15.8	344
9	180	1	14.8	281
10	190	1	14.6	270
11	140	2	16.8	284
12	160	2	15.0	363
13	180	2	14.5	298
14	190	2	14.3	280
15	140	3	17.4	298
16	160	3	14.6	380
17	180	3	14.3	308
18	190	3	13.8	283
19	140	4	16.5	313
20	160	4	14.5	394
21	180	4	14.0	326
22	190	4	13.5	291
23	140	5	16.0	324
24	160	5	17.3	410
25	180	5	13.7	372
26	190	5	13.1	354
27	140	6	15.5	450
28	160	6	14.1	430
29	180	6	13.4	482
30	190	6	12.8	348
31	140	7	14.9	325
32	160	7	13.3	444
33	180	7	13.0	430
34	190	7	12.1	364
35	140	8	14.2	510
36	160	8	13.1	416
37	180	8	12.2	408
38	190	8	11.4	344
39	140	9	13.3	371
40	160	9	12.8	346
41	180	9	11.2	338
42	190	9	10.5	308

Presented below are the results of the analysis of the as-cast and quenched at various temperatures at different times, plotted ultimate tensile UTS (MPa) against aging temperature in degrees Celsius.

Figure 3 is a condensed and multiferous bar chart plot showing the ultimate tensile strength of Al 2024 at the conditions of the as-cast, quenched, and aged for various aging temperatures and aging times. The Al 2024, in the as-cast condition, has an ultimate tensile strength of 185MPa. The optical microstructure (OM) of the as-cast condition is shown in Figure 4.

The analysis of the results, as presented in Figure 3, indicated that the Al 2024 responded positively to the aging heat treatment as its ultimate tensile strength was significantly improved at different aging temperatures and aging times. It showed an increase in the ultimate tensile strength of Al 2024 after being solution heat-treated and quenched in water. This increase is due to the retardation of the diffusion process during quenching. This agrees with the by Lewandowska et al., [27]. The optical microstructure (OM) of Al 2024 as cast and solutionized at 5500 °C for 2 hr quenched in water are shown in Figure 3. The quenched Al 2024 recorded an ultimate tensile strength of 199 MPa, which, according to Equation (3), represents an increase of 7.6% from the as-cast value.

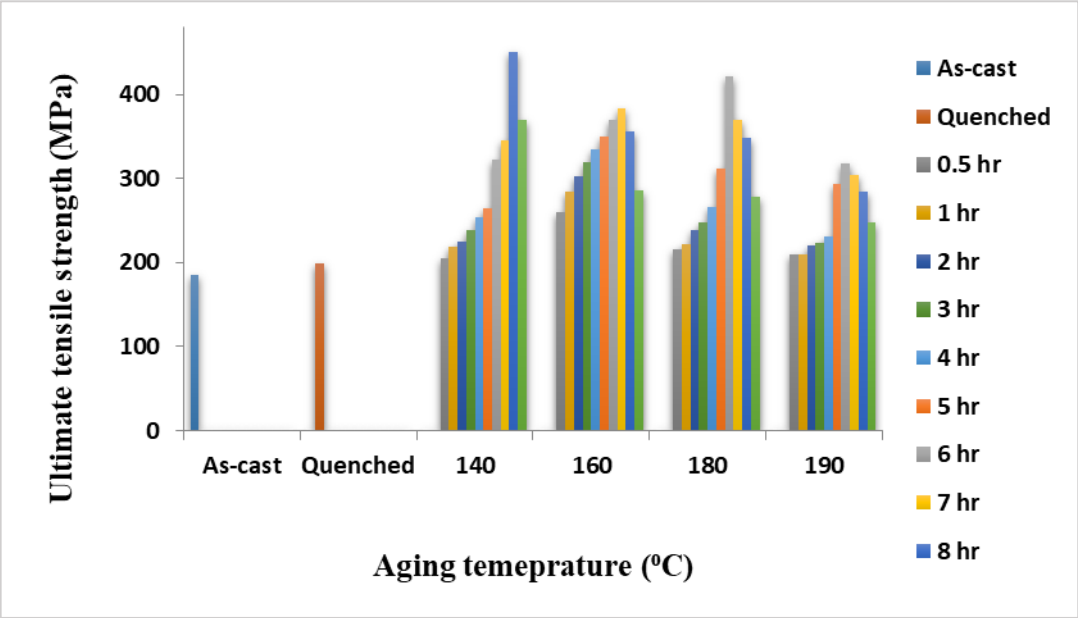

Figure 3: Effects of aging temperature and time on the ultimate tensile strength of Al 2024

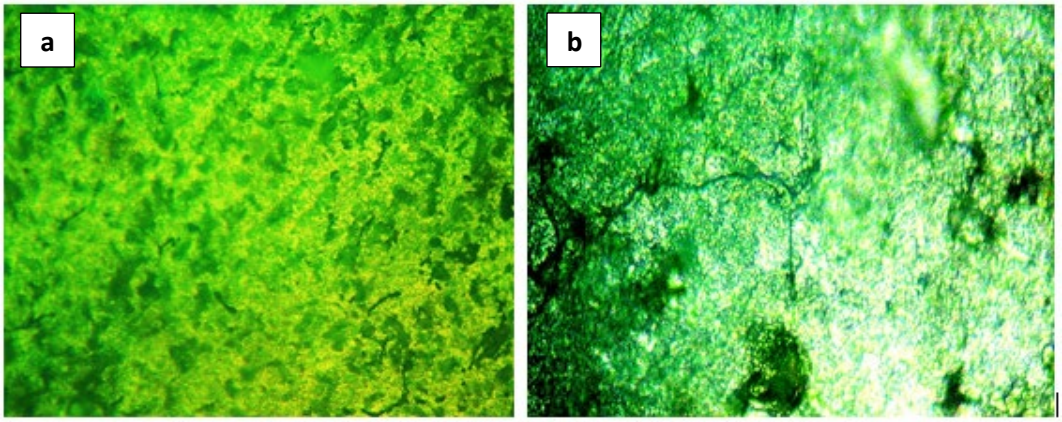

Figure 4: (a) As-cast OM of Al 2024 and (b) Quenched in water OM of Al 2024

2.5 Optical Microstructure Al 2024

Figures 4, 5, and 6 present the optical microstructure of Al 2024, revealing coarse grains of the solid solution matrix and bright disparities associated with intermetallic phases. These intermetallic phases are precipitated at grain boundaries and have different morphologies and dark disparities. Some of the intermetallic phases of AlCuMnMg alloy have a coarse plate-like morphology. This microstructure has an average grain size range of 30µm to 56µm. At the same time, the AlCuMnMg alloy aged treated containing phases at recognized different times appears as elongated grains parallel to the direction of rolling, while its morphology of plate-like precipitate is completely changed to fine particles. Figure 4 (a) illustrates the microstructure of the as-cast condition, showing finer precipitates along the grain boundaries compared to the quenched condition depicted in Figure 4 (b). Figure 5 (a) represents aging at 140 °C for 0.5 hr, where lattice formation has induced an increase in ultimate tensile strength (UTS). The precipitates at the grain boundaries are fine but not as fine as those observed in the as-cast condition. Figure 5 (b) shows aging at 140 °C for 7 hr, revealing slightly coarser particles along the grain boundaries, attributed to the increased aging time and temperature. In Figure 5(c), aging at 140 °C for 8 hr results in further particle coarsening due to the extended aging duration.

Figure 6 (a) demonstrates aging at 160 °C for 7 hr, where coarser particles are observed at the grain boundaries, corresponding to an increase in UTS due to the higher aging temperature and time. Figure 6 (b), aged at 160 °C for 8 hours, shows even coarser particles due to the prolonged aging duration. Conversely, Figure 6 (c), aged at 180 °C for 6 hours, exhibits finer particle sizes along the grain boundaries, resulting from the higher temperature combined with a shorter aging time. Finally, Figure 6 (d), aged at 190 °C for 6 hours, shows finer precipitate particles along the grain boundaries, corresponding to an increase in UTS.

Presented below are values of the ultimate tensile strength of 205 MPa, 260 MPa, 216 MPa, and 209 MPa at aging temperatures of 140 °C, 160 °C, 180 °C, and 190 °C, for 0.5, 6, 7, 8 hr, were recorded representing 10.9%, 40.5%, 16.8% and 13.0%, increases from the as-cast value respectively, using Equation (5). The optical microstructures (OM) of Al 2024 aged at 140 °C for 0.5 hr, is shown in Figure 5.

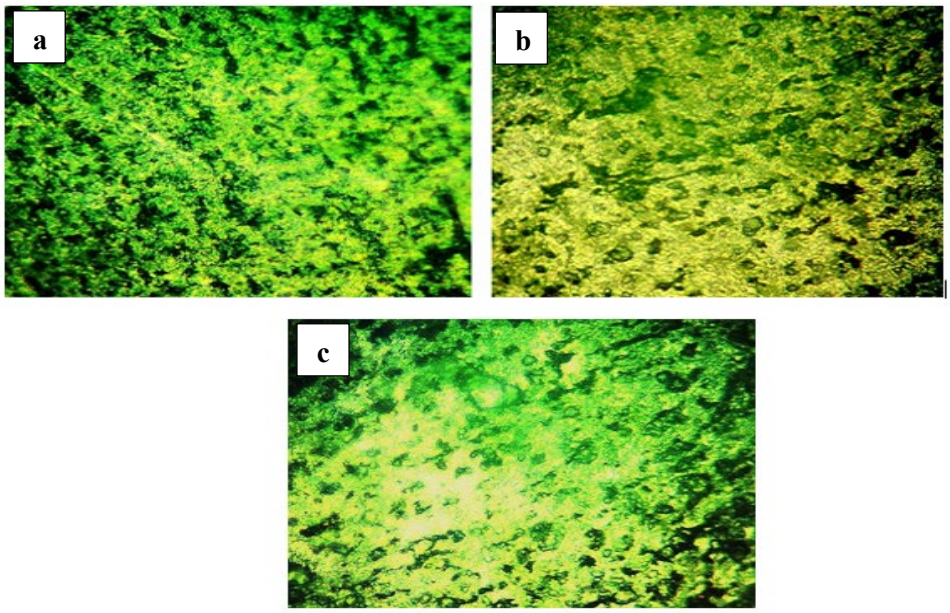

Figure 5: (a) OM aged at 140 °C for 0.5 hr, (b) Aged at 140 °C for 7 hr, and (c) Aged at 140 °C for 8 hr, of Al 2024

The coherent lattice phenomenon induced the improvement in ultimate tensile strength. Thus, the distortion of the coherency of the migrated solute atoms with the matrix lattice structure, which resulted in the interference and impediment to the movement of dislocations, increased the ultimate tensile strength during the aging process [28]. At the aging temperature of 140 °C, the Al 2024 recorded an overall maximum tensile strength of 510 MPa at 8 hr aging time, representing a 175.7% increase from the as-cast value. Also, at 160 °C, it recorded a maximum tensile strength of 430 MPa, representing a 132.4% increase, and at 6 hr aging time. In contrast, at 180 °C aging temperature and 6 hr aging time, it recorded an overall and semi-maximum ultimate tensile strength of 482 MPa, representing a 160.5% increase from the as-cast value, using Equation (5). The respective optical microstructures (OM) are shown in Figure 6.

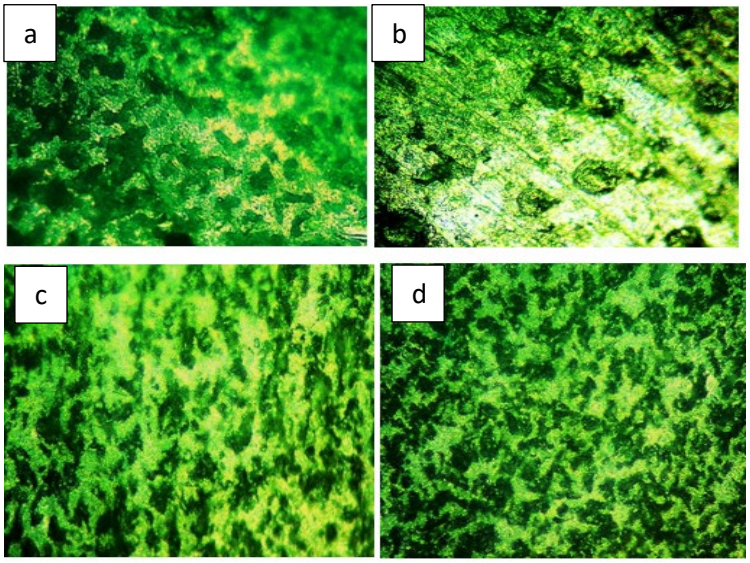

Figure 6: OM of Al 2024 (a) Aged at 160 °C for 7 hr, (b) Aged at 160 °C for 8 hr, (c) Aged at 180 °C for 6 hr, and (d)Aged at 190 °C, for 6 hr

Furthermore, at the aging temperature of 190 °C, the peak aging time is 6 hr with the ultimate tensile strength of 348 MPa, representing an 88.1% increase from the as-cast value, also using Equation (5). The respective optical microstructures (OM) are also shown in Figure 6 at the bottom right. Generally, drops in the ultimate tensile strength beyond the peak aging times can be attributed to the precipitated incoherent coarse secondary phases in the alloy structure. This is also observed in their work on heat treatment of AL 2024 [29].

3. Conclusion

The work was to increase the mechanical properties of Al 2024 alloy using aging heat treatment of the composite. The ultimate tensile strength of the as-cast increased from 185 MPa to 199 MPa, representing a 7.6% increase after solutionizing and quenching. This was induced by the retardation of the diffusion process and the presence of fine grains in the quenched

sample. Thereafter, improvement in the ultimate tensile strength progressively continued. At 190 °C aging temperature, the peak value of 348 MPa, representing an 88.1% increase of the as-cast value, was recorded at 6 hr aging time. The drops in ultimate tensile strength values outside the peak aging time of 6 hr were attributed to the precipitation of incoherent and coarse secondary phases in the alloy structure. There were further increases in the values of the ultimate tensile strength at various aging temperatures and aging times, culminating in 482 MPa as the semi-maximum overall value at 180 °C and 6 hr aging temperature, representing a 160.5% increase of the as-cast value. Meanwhile, 510 MPa was recorded as the overall maximum ultimate tensile strength at 140 °C and 8 hr aging time. Representing a 175.7% increase in the as-cast value. This increased the mechanical property of Al 2024, and it's so recommended for application in lightweight machines and equipment with respect to ultimate tensile strength.

Nomenclature

A	Area (mm^2)
BL	Bottom left
BR.	Bottom right
hr.	hour
KN	kilo-newton
Mpa	megapascal
Oc.	Degree Celsius
OM	Optical Microstructure
TR	Top right
TL.	Top left
UTS.	Ultimate Tensile. Strength (mpa)

Author contributions

Conceptualization, **B. Iyida**. **A. Nwankwo,** and **T. Onah**; data curation, **A. Nwankwo**.; formal analysis, **A. Nwanwko**.; investigation, **B. Iyida**.; methodology, **T. Onah**; project administration, **A. Nwankwo**, resources**, B. Iyida**.; software, **A. Nwankwo**.; supervision, **T. Onah**.; validation**, B. Iyida, A. Nwankwo**. and **T. Onah**.; visualization, **A. nwankwo**.; writing—original draft preparation, **B. Iyida**.; writing—review and editing, **T. Onah**. All authors have read and agreed to the published version of the manuscript.

Funding

This research received no specific grant from any funding agency in the public, commercial, or not-for-profit sectors.

Data availability statement

The data that support the findings of this study are available on request from the corresponding author.

Conflicts of interest

The authors declare that there is no conflict of interest.

References

[1] Y. Q. Chen, S. P. Pan, S. W. Tang, W. H. Liu, C. P. Tang, and F. Y. Xu, Formation Mechanisms and Evolution of Precipitate-free zones at Grain Boundaries in an Al-Cu-Mg-Mn alloy during homogenization, J. Mater. Sci., 51 (2016) 7780-7792. https://doi.org/10.1007/s10853-016-0062-x

[2] Mengchao Liang, Liang Chen, Guoqun Zhao and Yunyue Guo; ,Effects of Solution Treatment on Microstructure and Mechanical Properties an of Naturally Aged EN AW 2024 Al alloy, Journals of Alloys and Compounds, 1 (2020) 2-5. https://doi.org/10.1016/j.jallcom.2020.153943

[3] I. N. Oguocha, Y. Jin and S. Yannacopoulos, Characterization of AA2618 Containing alumina Particles, Mater. Sci. Technol., 13 (1997) 173-181. https://doi.org/10.1179/mst/.1997.13.3.173

[4] N. D. Alexopoulos and M. Tiryakioglu, Relationship between Fracture Toughness and Tensile Properties of A357 Cast Aluminum Alloy, Metall. Mater. Trans., 40 (2009) 702-715.

[5] N. Kisaoglu and S. Aksoz, Effect of Aging heat treatment on Mechanical and Metallurgical properties of Al2024 reinforced with B4C/Sic/Tic Hybrid Composite produced by vacuum Infiltration Method, Trans. Indian Inst. Met., (2023) 3193-3200. https://doi.org/10.1007/s12666-023-02953-x

[6] J. R. Davies, ASM Handbook on Carbon and Alloy Steels, ASM International , 1996.

[7] Y. Chongxiang, Z. Liwen, L. Shulun and G. Huiju, Kinetic Analysis of the Austenite Grain Growth in GCr15 Steel, J. Mater. Eng. Perform., 19 (2009) 112-115. https://doi.org/10.1007/s11665-009-9413-y

[8] W. Xu, J. Liu, G. Luan and C. Dong, Temperature Evolution, Microstructures and Mechanical Properties of Friction Stir Welded Thick 2219-0Aluminium Alloy Joints, Mater Des., 30 (2009). https://doi.org/10. 1016/j.mats.2009.03.018

[9] N. D. Alexopoulos and S. P. Pantelakis, Evaluation of the effect of Variations in Chemical Composition on the Quality of Al-Si-Mg, Al-u an Al-Zn-Mg ast Aluminium Alloy, J. Mater. Eng. Perform., 12 (2003)196-205. https://doi.org/10.1361/105994903770343358

[10] N. D. Alexopoulos and S. P. Pantelakis, Quality Evaluation of A357 Cast Aluminum Alloy Specimens Subjected to Different Artificial. ageing Treatment, Mater. Des., 25 (2004) 419-430. https://doi.org/10.1016/j.matdes.2003.11.007

[11] I. J. Polmear, Light Alloy: Metallurgy of the Light Metals, Butterworth-Heinemann, 1995.

[12] B. Smoljan, Prediction of Mechanial Properties and Microstructure Distribution of Quenched an Tempered Steel Shaft, J. Mater. Process. Technol., 175 (2006) 393-397. https://doi.org/10.1016/j.jmatprotec.2005.04.068

[13] D. Jiang and C. Wang, Influence of Microstructure on Deformation Behaviour and Fracture Mode of Al-Mg-Si Alloys, Mater. Sci. Eng. A., 352 (2003) 29-33. https://doi.org/10.1016/s0921-5093(02)00456-2

[14] W. D. Callister, Materials Science and engineering, New York: John Wiley and Sons, 1997.

[15] G. E. Totten, G. M. Webster and C. E. Bates, Quenching Handbook of Aluminum Physical Metallurgy an Processes, vol. 1, Florida: CRC press, Boca Raton, 2003.

[16] Y. Yunhe, L. Zheng-dong, L. Zhen, C. Zheng-zong, B. Han-sheng, Z. Chi and Z. Yang, Characterization an Numerical Simulation of Nucleation-Growth-Coarsening Kinetic of precipitation in G115 Martensitic heat resistance Steel during long-term Aging, J. Iron. Steel Res. Int., 30 (2022) 1-12. https://doi.org/10.1007/s42243-022-00854-9

[17] B. U. Iyida, A. M. Nwankwo and T. O. Onah, Parametric Effecton the Coefficient of Friction on a Noval Composite Material for Automobile Brake Linning, Int. Res. J. multidiscip. Technovation, 5 (2023) 12-19. https://doi.org/10.54392./irjmt.2342

[18] E. C. Rollanson, Metallurgy for Engineers, London: Edward Arnold ltd, 1998.

[19] A. Belhocine and M. Bouchetara, Temperature and Thermal. Stresses of vehicles Grey cast brake, E. J. res. technol., 11 (2013) 671-682. https://doi.org/10.1016/s1665-6423(13)71575-x

[20] A. Made, Hardness Improvement of Aluminum Alloy 2024 t3 After Artificial Aging Treatment, in Material Science: International conference on design, Energy, materials and manufacture engineering 539, Bali, Indonesia, (2019). https://doi,org/10.1088/1757-899x/539/1/012004

[21] C. E. Bates, G. T. Totten and G. M. Webster, Cooling Curve and Quench Factor Characterization of 2024 and 7075 Aluminum Bar Quenched in Type 1 Polymer Quenchant, 29 NY: CRC press, (1998) 1-3. https://doi.org/10.1615/HEATTRANSRES.V2g./1-3.160

[22] A. M. Nwankwo , T. O. Onah and O. M. Egwuagu, Determination of Impingement Cooling Fluid Temperature-Time profile for Extracted Tiger-Nut Juice (Cyprus Esculentus) by Lumped Thermal Mass Analysis, Eng. Technol. J., 41 (2023) 142-150. https://doi.org/10.30684/etj.2022.134483.1239

[23] Z. Ruixiao and M. Chaoli, Novel Fabrication of Bulk Fine-grained Al-u-Mg Alloy with Suprior Mechanial Properties, Adv. Eng. Mater., 18 (2016) 1027-1035. https://doi.org/10.1002/adem.201500450

[24] J. J. Williams, G. Piotrowski, R. Saha, and N. Chawla, Effects of Overaging and Particle Size on Tensile Deformation and Fracture of Particle-reinforced Aluminum Matrix Composite, Metall. Mater. Trans., 33 (2002) 3861-3869. https://doi.org/10.1007/s11661-002-0258-3

[25] A. M. Nwankwo , T. O. Onah and B. N. Nwankwojike, Assessment of liquid and gas Impingement Cooling Fluid with Numerical Solution for Better Steel Austempering, Springer J. Eng. Appl. Sci., (2022). https://doi.org/10.1186/s44147-022-00139-8

[26] S. Salem, T. Giulio, L. Ingvar and F. Svensson, Influence of Quench Rate on the Microstructures and Mechanical Properties of Aluminum alloys (A356 and A354), Int. Foundry Rese., 59 (2006)1-10.

[27] M. Lewandowska, H. Garbacz, W. Pachla, A. Mazur and K. J. Kurzydlowski, Grain Refinement in Aluminum and the Aluminum Al-Cu-Mg-Mn Alloy by Hydrostatic Extrusion, Mater. Sci., 23 (2005) 279.

[28] E. O. Obidiegwu, H. E. Mgbemere, E. F. Ochulor and P. A. Ajayi, Characteristics of train brake block composite reinforced with Aluminum dross, Niger. J. Technol., 39 (2020) 1123-1130. https://doi.org/10.4314/njt.v39i4.20

[29] A. M. Nwankwo , B. N. Nwankwojike and T. O. Onah, Analysis of Existing Temperature-Time Profile of Jet Impingement Cooling System for Steel Production, Am. J. Eng. Res., 11 (2022) 113-120.